Micron 78 (2015) 67–72

Contents lists available at ScienceDirect

Micron

journal homepage: www.elsevier.com/locate/micron

Quantifying mean inner potential of ZnO nanowires by off-axis electron holography

Yong Ding[a,*], Yuzi Liu[b], Ken C. Pradel[a], Yoshio Bando[c], Naoki Fukata[c], Zhong Lin Wang[a]

[a] School of Materials Science and Engineering, Georgia Institute of Technology, Atlanta, GA 30332-0245, United States
[b] Center for Nanoscale Materials, Argonne National Laboratory, 9700 South Cass Avenue, Argonne, IL 60439, United States
[c] International Center for Materials Nanoarchitectonics, National Institute for Materials Science, 1-1 Namiki, Tsukuba 305-0044, Japan

ARTICLE INFO

Article history:
Received 29 June 2015
Received in revised form 17 July 2015
Accepted 20 July 2015
Available online 26 July 2015

Keywords:
Off-axis electron holography
Mean inner potential
ZnO
Convergent beam electron diffraction

ABSTRACT

Off-axis electron holography has been used to quantitatively determine the mean inner potential of ZnO. [0 0 0 1] grown ZnO nanowires with hexagonal cross-sections were chosen as our samples because the angle between the adjacent surfaces is 120°, as confirmed by electron tomography, so the entire geometry of the nanowire could be precisely determined. The acceleration voltage of the transmission electron microscope was accurately calibrated by convergent beam electron diffraction (CBED)–higher-order Laue-zone (HOLZ) analyses. ZnO nanowires were tilted away from zone-axis to avoid strong dynamical diffraction effect, and the tilting angles were determined by CBED patterns. Our experimental data found a mean inner potential of ZnO as 14.30 ± 0.28 V.

1. Introduction

ZnO is not only a great semiconducting material, but also a good piezoelectric material owing to its lacking of inversion symmetry in its crystal structure (Albertsson et al., 1989). By combining piezoelectric with its semiconductor properties, ZnO and other Wurtzite structured materials have shown novel fundamental phenomena and device applications, leading to increasing interest in the emerging field of "piezotronics" since it was first proposed in 2006 (Gao and Wang, 2007; He et al., 2007; Wang, 2007; Wang and Song, 2006). The deformation induced piezoelectric polarization, and piezoelectric potential, play a strong role in determining its electrical transport properties. A better understanding of the piezoelectric potential distribution and its stability can help to optimize the device's performance. Off-axis electron holography is a suitable approach to explore the detailed electric potential distribution around nanomaterials at a high spatial resolution (Chung and Rabenberg, 2006; Völkl et al., 1999; Gatel et al., 2013; Li et al., 2009; Liu et al., 2007; McCartney and Smith, 2007). In order to qualitatively map the piezoelectric potential inside ZnO nanostructure by off-axis electron holography, we need to know an accurate value of the mean inner potential (MIP) of ZnO, which is the volume average of the coulomb potential of ZnO solid and corresponds to the zero-order Fourier coefficient of the crystal potential (Völkl et al., 1999).

Theoretical *Ab initio* computations of the MIP of ZnO has been reported as 15.75 V (Schowalter et al., 2006), which contradicts the value of 16.19 V calculated using the JEMS software (Stadelmann, 1987). Experimentally, the MIP is determined by off-axis electron holography by measure the phase shift of the electron wave transmitted through the sample with respect to a reference wave that only propagates through the vacuum region. This phase difference $\Delta\Phi$ depends on the specimen thickness t and its MIP (V_0). It is given by (Reimer, 1984)

$$\Delta\Phi = C_E V_0 t \tag{1}$$

and

$$C_E = \frac{2\pi e}{\lambda E}\frac{E_0 + E}{2E_0 + E} \tag{2}$$

where e is the charge of electron, λ is the wavelength of incident electron, and E_0 and E are respectively, the kinetic and rest energy of the incident electron. The constant C_E can be determined if we know the operating voltage of the transmission electron microscope with high accuracy. If the sample thickness is known, then the MIP can be calculated using Eq. (1). Elfwing and Olsson (Elfwing and Olsson, 2002) used electron energy-loss spectra to measure the thickness of ZnO thin film, and received the MIP of ZnO as 21.0 ± 4.2 V. Using cylindrical ZnO nanorods, Müller et al. (Müller et al., 2005) determined the MIP of ZnO to be 15.9 ± 1.5 V. It has been reported that

* Corresponding author.
E-mail address: yong.ding@mse.gatech.edu (Y. Ding).

http://dx.doi.org/10.1016/j.micron.2015.07.008
0968-4328/

by choosing cleaved crystal wedges of known angle, the MIP can be accurately measured (Gajdardziska-Josifovska et al., 1993; Kruse et al., 2003; Li et al., 1999). For a sample of uniform V_0 and known wedge angle, Eq. (1) can be rearranged as:

$$V_0 = \frac{1}{C_E}\frac{d\Phi/dx}{dt/dx} \tag{3}$$

The change in phase with the position on the sample, $d\Phi/dx$ can be determined after reconstruction of an off-axis electron hologram. dt/dx is the lateral rate of thickness change. The local specimen thickness t in the electron-beam direction can be calculated from the wedge geometry of the specimen according to:

$$t = \frac{\tan((\theta/2)-\alpha)+\tan((\theta/2)+\alpha)}{\cos\beta}x \tag{4}$$

θ is the wedge angle, and α and β are the tilting angles as defined by the sketch shown in Fig. 1, which can be determined experimentally. By using this approach, the MIP of Si, MgO, GaAs and PbS have been measured with about 1% accuracy (Gajdardziska-Josifovska et al., 1993).

In this work, we chose hexagonal ZnO nanowires, which have fixed 120° wedges. The accelerating voltage of the transmission electron microscope was determined by convergent beam electron diffraction (CBED)–higher-order Laue-zone (HOLZ) analyses (Rao et al., 2004). The tilting angles of α and β were determined by its CBED pattern as well. Our measured MIP of ZnO is 14.30 ± 0.28 V.

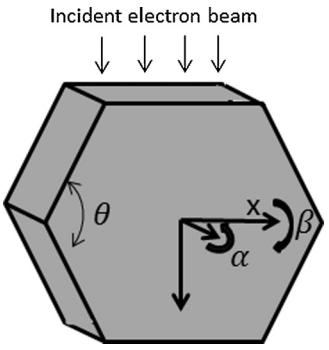

Fig. 1. Tilting geometry of a hexagonal sample under electron beam illumination.

2. Experimental

ZnO nanowires were synthesized using a vapor deposition approach (Wang et al., 2006). A FEI Tecnai F30 super-twin field-emission-gun TEM equipped with both a single-tilt tomography holder from Fischione Instrument and FEI double-tilt holder was used to acquire the TEM images, convergent-beam electron diffraction (CBED) patterns, and high-angle annular dark-field (HAADF) scanning transmission electron microscopy (STEM) images. The phase shift was retrieved from hologram reconstruction with reference by using holoworks, a plugin for Gatan DigitalMicrograph. JEMS software from Dr. Stadelmann was used to do the CBED simulation.

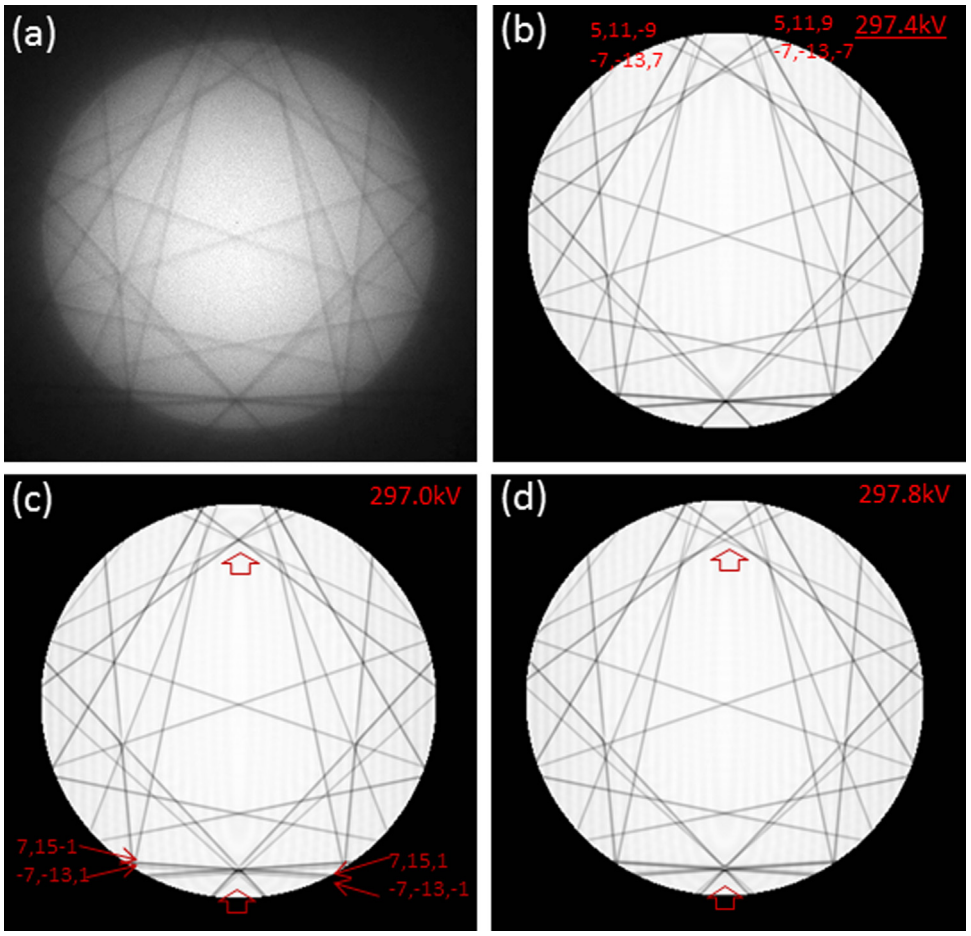

Fig. 2. (a) Experimental (0 0 0) disk for on-zone [2-10] CBED pattern in Si. (b), (c) and (d) Calculated ones corresponding to 297.4 kV, 297.0 kV and 297.8 kV operating voltages, respectively.

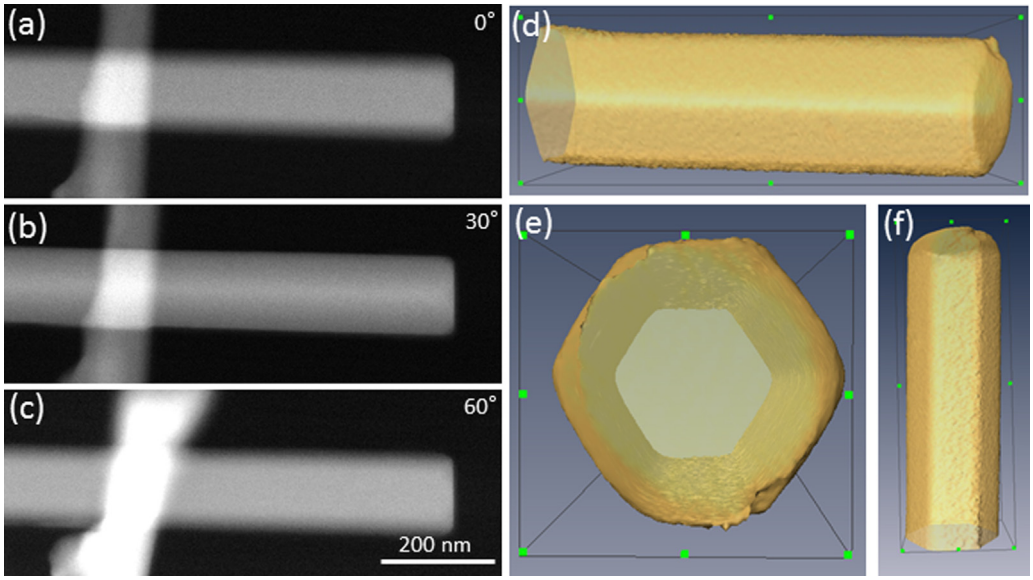

Fig. 3. (a)–(c) HAAD STEM images recorded at different tilting angles. (d)–(f) Reconstructed 3D structure of the ZnO nanowire shown in (a)–(c) from different orientations.

3. Results and discussion

In order to precisely measure the TEM operating voltage, we recorded a CBED pattern from a standard Si sample with electron beam parallel along the [2–10] zone axis. The positions of higher-order Laure-Zone (HOLZ) lines in the (0 0 0) disk can be seen clearly in Fig. 2(a). Fig. 2(b)–(d) gives the simulated CBED patterns by using the JEMS software (Stadelmann, 1987). The positions of HOLZ lines

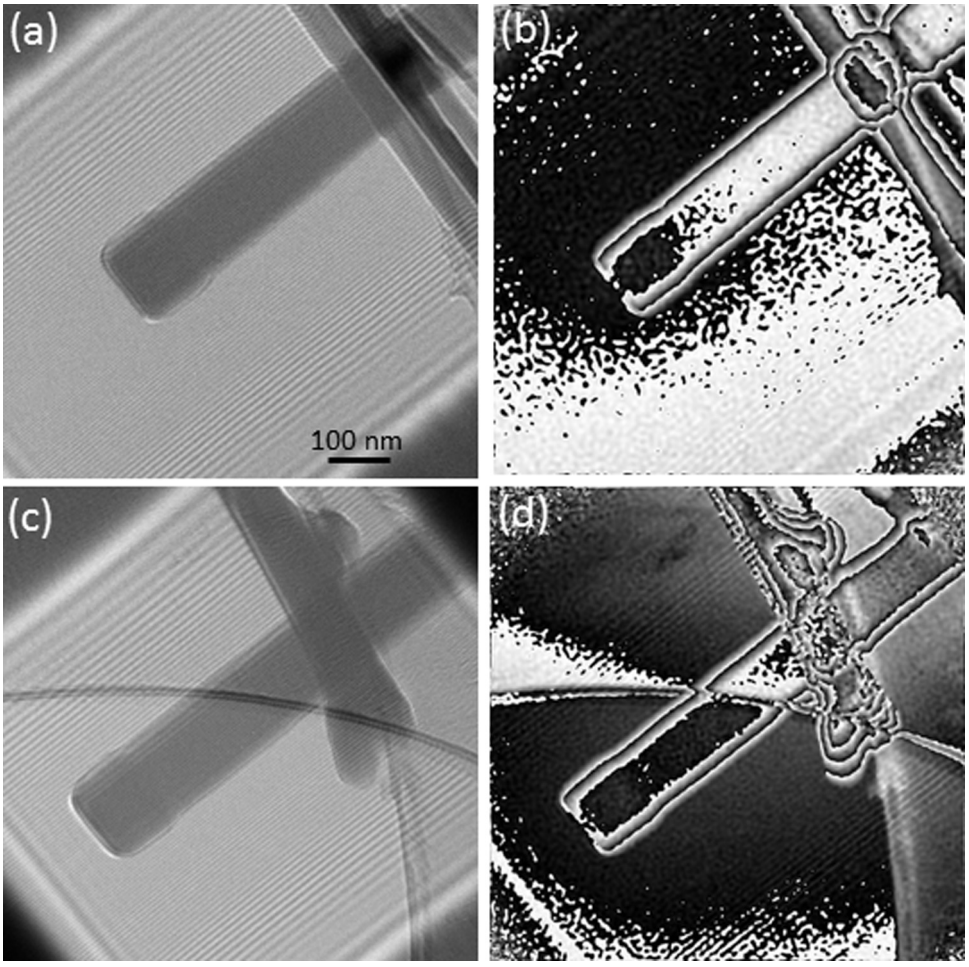

Fig. 4. (a) and (c) Electron holograms recorded from the same ZnO nanowire at 0° and 60° tilting angles. (b) and (d) Calculated phase images from (a) and (c), respectively.

of (7, 15, −1), (−7, −13, 1), (7, 15, 1) and (−7, −13, −1) in the bottom and (5, 11, −9), (5, 11, 9), (−7, −13, 7) and (−7, −13, −7) in the top are sensitive to the operating voltages as marked in Fig. 1(b)–(d). The best matched CBED pattern gives the operating voltage as 297.4 kV. The accuracy of the measured operating voltage is ±0.2 kV based on a series simulation.

The hexagonal shape of ZnO nanowires has been confirmed by electron tomography as shown in Fig. 3. A tilt series HAADF STEM images was acquired over the tilt range from −70° to 70° using *Xplore 3D* software (FEI Company) by a step of 2°. Three typical HAADF STEM images are displayed in Fig. 3(a)–(c), respectively, corresponding to 0°, 30° and 60° tilt angles. The detailed electron tomography reconstruction procedure can be found in a related reference (Ding et al., 2013). Fig. 3(d)–(f) gives the 3D view of the reconstructed nanowire from different orientations. Although the six surfaces are not in the same size, all the measured angles between joint surfaces are verified as 120°.

Off-axis electron holography investigation was carried out in Lorentz operating mode to provide a larger electron beam interference region, in which the whole ZnO nanowire was covered. A positive voltage of 236 V was applied to the filament of the biprism, which is mounted in one of the selected area apertures. The holograms were recorded by a CCD camera with a size of $2k \times 2k$ pixels.

Fig. 4(a) shows an electron hologram from the same ZnO nanowire as displayed in Fig. 3. The measured fringes spacing in the hologram without a specimen is about 2.3 nm. So the spatial resolution of the reconstructed phase image is about 4.6–6.9 nm because every detail resolved after reconstruction had to be sampled with 2–3 hologram fringes. The hologram is taken with the axial direction of the ZnO nanowires parallel to the biprism. The phase image in Fig. 4(b) is reconstructed from the hologram in Fig. 4(a) combined with a reference hologram (not shown here), in which the nanowire was retracted from the hologram very carefully to ensure that the optical parameters of the microscope did not change. After the sample was tilted 60° along the axis direction of the nanowire, we recorded another hologram from the same area as displayed in Fig. 4(c). Fig. 4(d) gives the reconstructed phase image from Fig. 4(c). The phase images in Fig. 4(b) and (d) are displayed as an equiphase pseudocontour image. The 2π phase contours are straight, parallel to the side surface of the nanowire. The off-color tip of the nanowire in Fig. 4 is due to the carbon contamination. The tip area was used to adjust the focus condition of each HAADF STEM image for electron tomography. So the carbon contamination is so obvious. There is less contamination in other area. Because we calculate the MIP based on the slope of the phase profile, or only the projected linear change of the thickness matters, the uniformly coated carbon film on the surface will not affect the phase change in Eq. (3).

The line profiles in Fig. 5(a) and (b) were extracted from the phase unwrapping images from Fig. 4(b) and (d), respectively. The plots in Fig. 5 show the 50-pixels averaged phase line profiles from the highlighted rectangles in their inserted unwrapping phase images. The phase from vacuum area has been calibrated. The smoothness of the phase line profiles with increasing thickness at the two side edges of the nanowire confirms the high quality of the hologram recording and reconstruction process. As indicated in Fig. 1, the hexagon shaped ZnO nanowire was tilted small angles α and β along the <0 0 0 1> and <2-1-10> directions, respectively. The thickness profile have five segments or three segments while $\alpha = 0$. The middle one is a flat plateau. The outside is two slopes from the projection of the two apexes. And in between there are another two segments with slope different from the outside segments. Since the tilt angle is just several degrees, those two extra segments are relatively much small and will not be considered in following discussion. Because of the truncated edges of the ZnO nanowire, we choose the middle part of the slope ~40 nm in width to do the

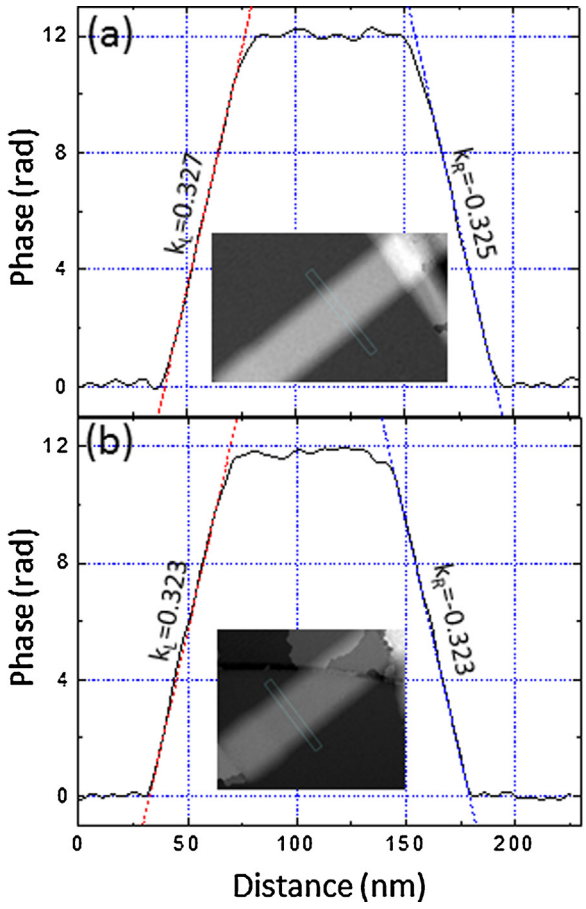

Fig. 5. Averaged phase line profiles taken from boxed regions in the inserted unwrapping phase images.

linear fitting. As a result, the fitting to the phase line profile in Fig. 5(a) yields two slopes of $|d\Phi/dx| = 0.327$ (left) and 0.325 (right) rad/nm. The statistical error for the least-squares fit is ~0.00073 rad/nm. The both fitting slopes in Fig. 5(b) are 0.323 rad/nm.

In order to avoid the strong dynamical diffraction effect, the nanowire in Fig. 4 has been tilted several degrees away from the <01-10> zone axis. As we know that the ZnO nanowire grows along the [0001] direction, the tilting angles α and β as depicted in Fig. 1 can be considered as tilting along the <0 0 0 1> and <2-1-10> directions respectively. Fig. 6(a) and (c) gives the CBED patterns recorded form the nanowire before and after 60° tilting, while Fig. 6(b) and (d) are the simulated CBED patterns using JEMS software. The tilting angles α and β revealed by the simulation is 1.59°, 0.87° as displaced in Fig. 6(a), they are 2.23° and 0° in Fig. 6(c).

Considering the operating voltage is 297.4 ± 0.2 kV, we have the $C_E = 0.00654\ \text{rad}(V_{\text{nm}})^{-1}$ with an error of ~0.02%. Based on the values of α, β, C_E and the slopes of 0.327, 0.325 and 0.323 rad/nm shown in Fig. 5, we got the MIP of ZnO as $V_0 = 14.38$ V, 14.30 V and 14.17 V according to Eqs. (3) and (4). We measured the MIP from 5 different single nanowires. Considering the high accuracy of our measurements of the operating voltage and slope of the phase profile, they only contribute to ~0.1% error. Because the experiment was carried out in Lorentz mode, the measured length is the major contributor to the error. The magnification in Lorentz mode was calibrated by a standard Au coated carbon grid, in which the diffraction parallel line gratings have fixed spacing of 462.9 nm. By counting all the possible errors, we have a final MIP of $V_0 = 14.30 \pm 0.28$ V.

The MIP can also be calculated by using Eq. (1) if the sample thickness can be measured. In our experiment, each hexagonal ZnO

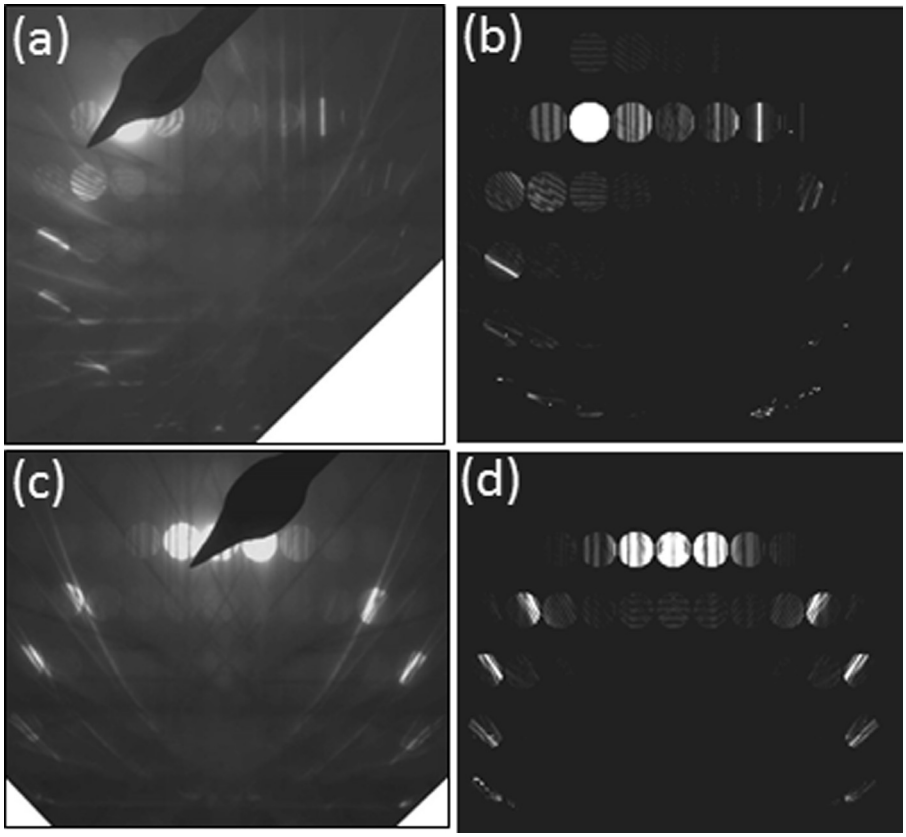

Fig. 6. Comparison of experimental and simulated CBED patterns at 0° and 60° tilting angles.

nanowire is enclosed by six {01-10} surface planes, two of them are parallel to each other, like the top and bottom surfaces as displayed in Fig. 3(e). Therefore, the overlapping projection area of these paired surfaces in the incident electron beam direction has the same thickness. The phase change corresponding to such thickness can be read out from the platform in its phase profile curve. It is $\Delta\Phi = 12.03 \pm 0.21$ rad in Fig. 5(a). The thickness can be retrieved from electron tomography reconstruction as shown in Fig. 3. Due to the limited resolution of electron tomography, the projected thickness from the top-bottom surface area is calculated as 134 ± 10 nm. Then the calculated MIP is $V_0 = 13.73 \pm 1.24$ V according Eq. (1).

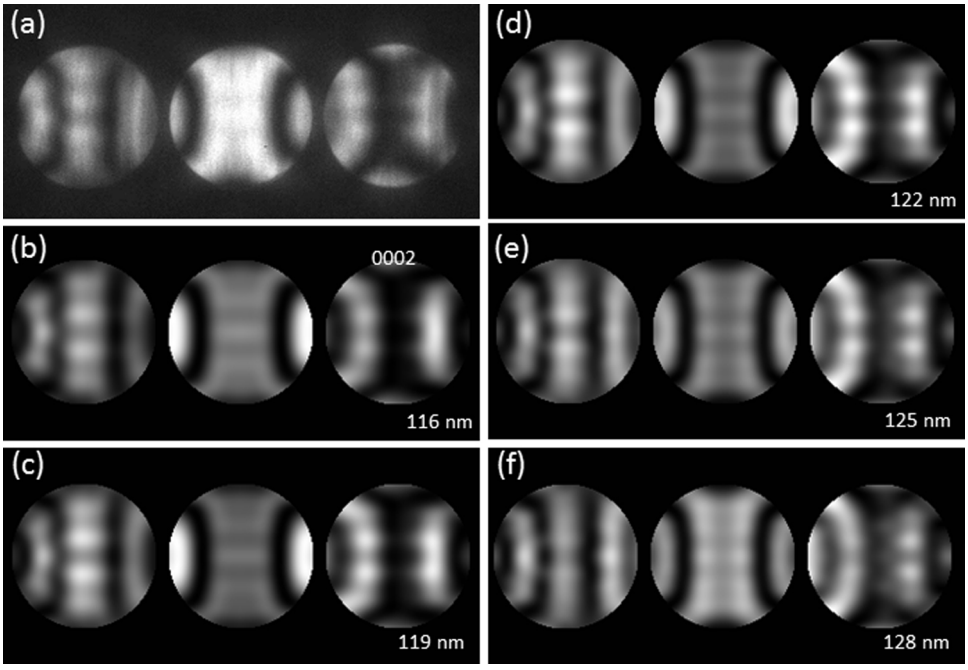

Fig. 7. Experimental and simulated [01-10] CBED patterns used to estimate the sample thickness.

The projected thickness from the top-bottom surfaces area can be measured from CBED pattern displayed in Fig. 7(a). The thickness of 122 ± 6 nm was achieved by matching the experimental pattern with the simulated ones shown in Fig. 7(b)–(f). The CBED pattern in Fig. 7(a) was taken at the electron beam parallel with the zone axis direction. Considering the hologram was taken by a small angle departure away from the zone axis, total about 1.8°, the rectified projection thickness based on CBED pattern still gives 122 ± 6 nm. It is much smaller than which extracted from electron tomography. It may be due to the carbon contamination layer on the surface of nanowire, which contributes extra mass contrast and affects the electron tomography results but not the CBED patterns. In such case, the MIP is $V_0 = 15.08 \pm 1.06$ V according Eq. (1).

By comparing the above three MIP data measured using different approaches, the one based on the fix-angle wedges gives higher accuracy with less than 0.1% error, while the ones based on the electron tomography reconstruction and CBED patterns give error ~9% and 7%, respectively. And furthermore, by measuring more nanowires, we find all the measured MIPs based on the fix-angle wedges approach stay in a small range (less than 0.30 V) close to 14.30 V, while other approaches by measuring sample thickness mentioned previously give bigger changes (2.00 V).

4. Conclusion

We have measured the mean inner potential ($V_0 = 14.30 \pm 0.28$ V) of ZnO from hexagonal nanowire samples at a high accuracy using off-axis electron holography operating in Lorentz mode. Each hexagonal ZnO nanowire gives two fixed 120° wedges suitable for electron holography measurement based on phase and thickness change slops instead of thickness which is hard to be measured accurately. In order to reduce the error, the dynamic diffraction effect was minimized by tilting the nanowires several degrees away from the <01-10> zone axis. The tilting angles were measured by comparing the experimental and computational CBED patterns. The operating voltage was determined by CBED–HOLZ analysis.

Acknowledgements

Research was supported by the National Science Foundation (DMR-1505319), and MANA, National Institute for Materials Science, Japan. This work was performed, in part, at the Center for Nanoscale Materials, a U.S. Department of Energy Office of Science User Facility under Contract No. DE-AC02-06CH11357.

References

Albertsson, J., Abrahams, S.C., Kvick, A., 1989. Atomic displacement, anharmonic thermal vibration, expansivity and pyroelectric coefficient thermal dependences in Zno. Acta Crystallogr. B 45, 34–40.
Chung, J.H., Rabenberg, L., 2006. Mapping of electrostatic potentials within core–shell nanowires by electron holography. Appl. Phys. Lett. 88, 013106.
Ding, Y., Zhang, F., Wang, Z.L., 2013. Deriving the three-dimensional structure of ZnO nanowires/nanobelts by scanning transmission electron microscope tomography. Nano Res. 6, 253–262.
Elfwing, M., Olsson, E., 2002. Electron holography study of active interfaces in zinc oxide varistor materials. J. Appl. Phys. 92, 5272–5280.
Gajdardziska-Josifovska, M., Mccartney, M.R., Deruijter, W.J., Smith, D.J., Weiss, J.K., Zuo, J.M., 1993. Accurate measurements of mean inner potential of crystal wedges using digital electron holograms. Ultramicroscopy 50, 285–299.
Gao, Y., Wang, Z.L., 2007. Electrostatic potential in a bent piezoelectric nanowire. The fundamental theory of nanogenerator and nanopiezotronics. Nano Lett. 7, 2499–2505.
Gatel, C., Lubk, A., Pozzi, G., Snoeck, E., Hytch, M., 2013. Counting elementary charges on nanoparticles by electron holography. Phys. Rev. Lett. 111, 025501.
He, J.H., Hsin, C.L., Liu, J., Chen, L.J., Wang, Z.L., 2007. Piezoelectric gated diode of a single ZnO nanowire. Adv. Mater. 19, 781–784.
Kruse, P., Rosenauer, A., Gerthsen, D., 2003. Determination of the mean inner potential in III–V semiconductors by electron holography. Ultramicroscopy 96, 11–16.
Li, J., McCartney, M.R., Dunin-Borkowski, R.E., Smith, D.J., 1999. Determination of mean inner potential of germanium using off-axis electron holography. Acta Crystallogr. A 55, 652–658.
Li, L.Y., Ketharanathan, S., Drucker, J., McCartney, M.R., 2009. Study of hole accumulation in individual germanium quantum dots in p-type silicon by off-axis electron holography. Appl. Phys. Lett. 94, 232108.
Liu, Y.Z., Han, X.D., Zhang, Z., 2007. Potential mapping of ZnO by off-axis electron holography. Philos. Mag. Lett. 87, 103–111.
McCartney, M.R., Smith, D.J., 2007. Electron holography: phase imaging with nanometer resolution. Annu. Rev. Mater. Res. 37, 729–767.
Müller, E., Kruse, P., Gerthsen, D., Schowalter, M., Rosenauer, A., Lamoen, D., Kling, R., Waag, A., 2005. Measurement of the mean inner potential of ZnO nanorods by transmission electron holography. Appl. Phys. Lett. 86, 154108.
Rao, D.V.S., Balamuralikrishnan, R., Muraleedharan, K., 2004. Accurate determination of the voltage of a transmission electron microscope (TEM) by <0 1 2> CBED–HOLZ analyses using GaAs crystal. Bull. Mater. Sci. 27, 471–482.
Reimer, L., 1984. Transmission Electron Microscopy. Springer, Berlin.
Schowalter, M., Rosenauer, A., Lamoen, D., Kruse, P., Gerthsen, D., 2006. Ab initio computation of the mean inner Coulomb potential of wurtzite-type semiconductors and gold. Appl. Phys. Lett. 88, 232108.
Stadelmann, P.A., 1987. EMS – a software package for electron-diffraction analysis and Hrem image simulation in materials science. Ultramicroscopy 21, 131–145.
Völkl, E., Allard, L.F., Joy, D.C., 1999. Introduction to Electron Holography. Kluwer Academic/Plenum Publishers, New York.
Wang, Z.L., 2007. Nanopiezotronics. Adv. Mater. 19, 889–892.
Wang, Z.L., Song, J.H., 2006. Piezoelectric nanogenerators based on zinc oxide nanowire arrays. Science 312, 242–246.
Wang, X.D., Song, J.H., Summers, C.J., Ryou, J.H., Li, P., Dupuis, R.D., Wang, Z.L., 2006. Density-controlled growth of aligned ZnO nanowires sharing a common contact: a simple, low-cost, and mask-free technique for large-scale applications. J. Phys. Chem. B 110, 7720–7724.